CHAPTER 5

Determination of $^{233}Pa(2n_{th}, f)$ cross-section using a fission track technique

Published in:

1. H. Naik, **P. M. Prajapati** *et al., $^{233}Pa(2n_{th}, f)$ cross-section determination using a fission track technique,*, Eur. Phys. J A **47**, 100 (2011)

5.1 Introduction

In recent time, major effort has been directed to develop nuclear power generation based on the concept of fast reactors [1, 2], advanced heavy water reactors (AHWR) [3-6] and accelerator driven sub-critical systems (ADS) [7-10]. In AHWR, ^{232}Th-^{233}U is the primary fuel for power generation. On the other hand, ^{232}Th-^{233}U fuel in connection with ADS [7-10] is one of the possibilities for power generation besides transmutation of long-lived fission products (e.g. ^{93}Zr, ^{99}Tc, ^{107}Pd, ^{129}I & ^{135}Cs) and incineration of long-lived minor actinides (e.g. ^{237}Np, ^{240}Pu, ^{241}Am, ^{243}Am & ^{244}Cm) to solve the problem of radioactive waste. Thus, the concept of the energy amplifier (EA) [7-10] in the hybrid system is based on the thorium fuel cycle and a spallation neutron source in ADS. The ^{232}Th-^{233}U fuel in AHWR and ADS has an advantage over the present reactor based on uranium fuel from the point of production of thousand times less radiotoxic waste (long-lived minor actinides) in the former than the latter. In the thorium-uranium fuel cycle, the fissile nucleus ^{233}U is generated by two successive β-decays after a neutron capture by the fertile nucleus ^{232}Th. A schematic diagram of ^{233}U production from ^{232}Th is given below in Fig. 5.1 [11].

The production of ^{233}U is controlled by ^{233}Pa with a half-life of 26.967 days and thus the neutron induced fission/reaction and neutronics properties of the latter nucleus influence directly the inventory of the fissile material ^{233}U. Therefore, the knowledge on the neutron induced fission/reaction of ^{233}Pa is essential for the design of AHWR and ADS. So far sufficient data of neutron-induced (n, γ) reaction cross-sections [12, 13] and (n, f) cross-sections [14-18] of ^{233}Pa from direct and indirect measurements are available in the literature. From these data, it can be seen that ^{233}Pa has a very low fission cross-section of < 0.1 b [19] for low energy (0.025 eV) neutrons due to its higher fission threshold. On the other hand, it has a sufficiently high neutron absorption cross-section of 39.5 b [19] to produce ^{234}Pa, which can undergo fission by additional thermal neutron capture.

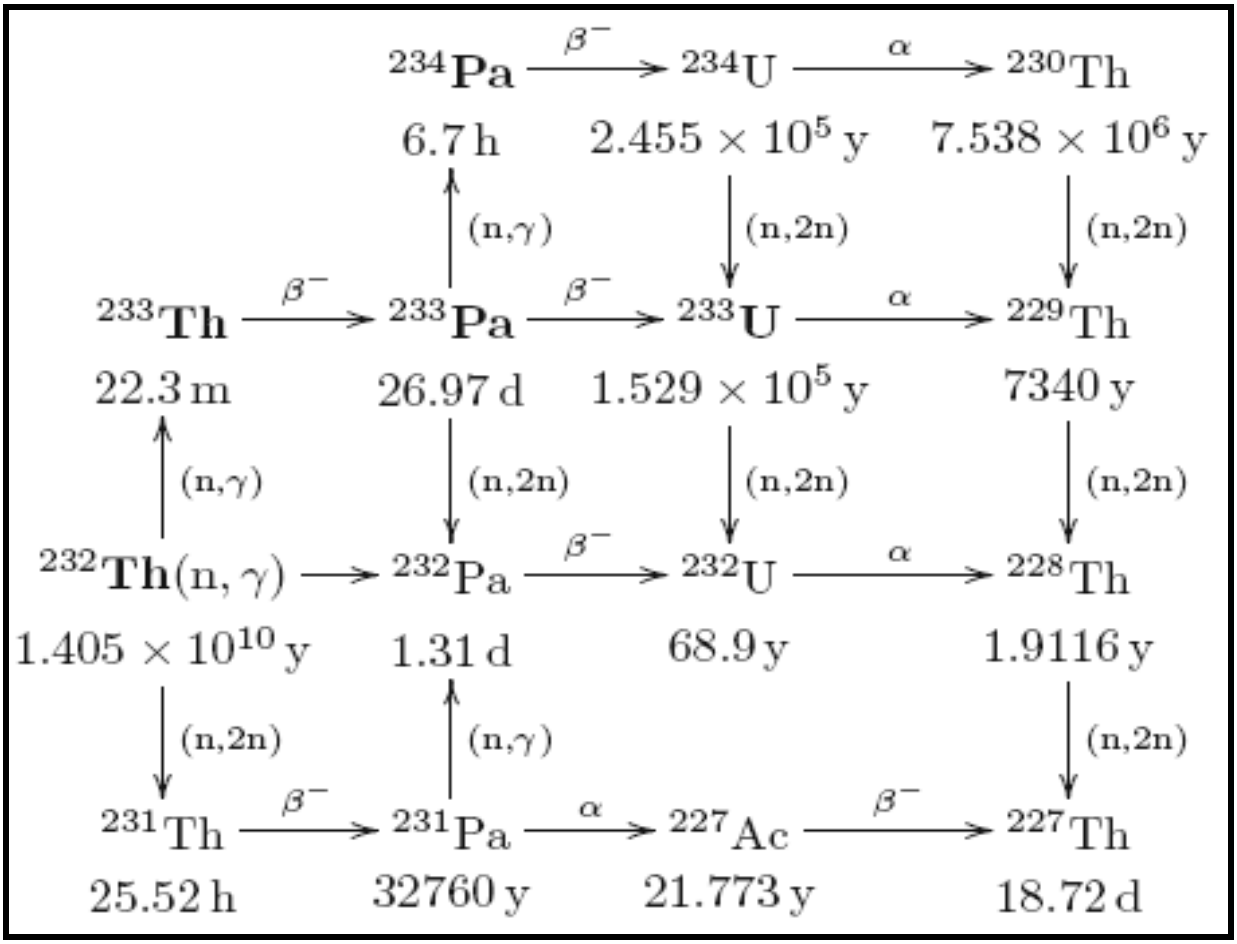

Fig. 5.1 A schematic diagram of ^{233}U production from ^{232}Th

A detailed literature survey indicates that there is no data available for the neutron induced fission cross-section of ^{234}Pa from direct or indirect measurements except the value of an upper limit quoted in Ref. [19]. This is because of the short half-life of 1.17 min for $^{234}Pa^{m}$ and 6.7 h for $^{234}Pa^{g}$ [11]. The ^{234}Pa(n_{th}, f) cross-section is expected to be lower compared to ^{232}Pa(n_{th}, f). This is because in another odd-Z fissioning system ^{244}Am(n_{th}, f) has a lower cross-section compared to ^{242}Am(n_{th}, f) [19] having a difference of two neutrons analogous to ^{234}Pa and ^{232}Pa. In case of the adjacent even-Z fissioning system ^{229}Th(n_{th}, f), the cross-section is lower than for ^{227}Th(n_{th}, f) [19-21]. However, in case of ^{235}U(n_{th},f) and ^{241}Pu(n_{th},f) the cross-section is comparable or slightly higher than for ^{233}U(n_{th},f) and ^{239}Pu(n_{th},f), respectively [19-21]. It is important to examine the above aspects in the fissioning systems ^{234}Pa(n_{th}, f) and ^{232}Pa(n_{th}, f) because of their importance in AHWR and ADS design. In view of this, the ^{234}Pa(n_{th}, f) (i.e. ^{233}Pa($2n_{th}$, f)) cross-section has been determined for the first time using a fission track technique.

5.2 India's first Nuclear reactor – APSARA

India's first nuclear reactor was APSARA. It was also the first nuclear reactor in Asia. APSARA went critical on August 4, 1956 at Bhabha Atomic Research Centre (BARC), Trombay, Mumbai. It heralded the arrival of India's nuclear energy programme. Dr. Homi Bhabha himself conceptualized the design of the reactor and it was built entirely by Indian engineers in a record time of about 15 months.

APSARA is a swimming pool type of reactor loaded with enriched Uranium fuel [22]. The core is suspended from movable trolley in a pool 8.4 M deep filled with de-mineralized light water. The pool walls are made of reinforced concrete 2.6 meter thick and 3 meter high and thereafter tapering to 0.7 meter thickness. The pool water serves as coolant, moderator and reflector besides providing shielding. The fuel is in the form of alloy with ^{235}U enrichment limited to 93% w/w [22]. Overall dimensions of fuel elements are 73 x 73 x 905 mm and a standard fuel element has 12 fuel plates. Each fuel plate consist of 0.5 mm thick Uranium Aluminum alloy meat clad with 0.5 mm thick Aluminum. The reactor is designed for a maximum power level of 1 MW_t operation and is normally operated up to 400 KW_t since most of the user needs are fulfilled at this power level. The average neutron flux available in the beryllium neutron source is used for reactor start-up.

APSARA has been extensively used for following R & D [22] since 1956:

1. Isotope production
2. Fission studies
3. Neutron activation analysis
4. Beam tube research
5. Biological application
6. Neutron radiography
7. Neutron detector testing
8. Shielding experiment
9. Studies on Radiation Stability of Reactor materials
10. Studies on chemical consequences of Nuclear Transformations in solids
11. Radiation damage and hardness studies
12. Bio-kinetics of Uranium and Thorium
13. Estimation of Trace levels

5.3 Experimental Details and Calculations

For the determination of $^{233}Pa(2n_{th}, f)$ cross-section, the experiment was carried out in APSARA reactor, B.A.R.C, Mumbai. The radiochemical separation of ^{233}Pa from irradiated Thorium Nitrate **($Th(NO_3)_4.4H_2O$)** was performed at Radiochemistry Division, Radiological Laboratory (RLG), B.A.R.C, Mumbai, India.

5.3.1 Radiochemical separation of ^{233}Pa from irradiated Thorium Nitrate ($Th(NO_3)_4.4H_2O$)

About 6 gm of thorium nitrate salt was wrapped with 0.025 mm thick aluminum foil and doubly sealed with alkathene. The target was kept inside a polypropylene capsule and irradiated for 8 h in the swimming pool type reactor APSARA at a neutron flux of $1.2x10^{12}$ n cm^{-2} s^{-1}. After sufficient cooling, the irradiated thorium nitrate salt was dissolved in 8 N HCl in a polyethylene container. Di-isobutyl carbinol (DIBC), procured from Aldrich, USA, was used as an extractant for the separation of ^{233}Pa [23] and quantitative stripping was achieved by 0.1 N HCl. Purity and amount of the final product was ascertained by a γ-ray spectrometric technique [24] using an energy and efficiency calibrated 80 cm^3 HPGe detector coupled to a PC-based 4K

channel analyzer and by following the decay profile. The resolution of the detector system during counting was 2.0 keV at the 1332.5 keV γ line of ^{60}Co. The standard source used for the energy and efficiency calibration was ^{152}Eu having γ-rays in the energy range of 121.8 keV to 1408.0 keV. The detector efficiency was 20 % at 1332.5 keV relative to a 3″ diameter x 3″ length NaI(Tl) detector. The γ-ray counting of the sample was done in live time mode. The dead time of the counting was kept less than 5% by placing the sample in a fixed geometry at a suitable distance from the detector. Typical γ ray spectrums of separated ^{233}Pa from irradiated thorium nitrate are given in Figs. 5.2 and 5.3. The seven different γ-lines of ^{233}Pa are clearly seen from Figs. 5.2 and 5.3. There are no other γ lines besides the x-rays (Fig. 3), which indicates the purity of the sample and absence of other fissile impurities. The radioactive decay of the ^{233}Pa sample was followed as a function of time to confirm the identity of nuclide ^{233}Pa which is shown in Fig. 5.4. Further, ^{233}Pa stock solution was evaporated to dryness several times with nitric acid to eliminate chloride. Finally, the Pa stock activity was stored in 6M HNO_3 in a polyethylene beaker.

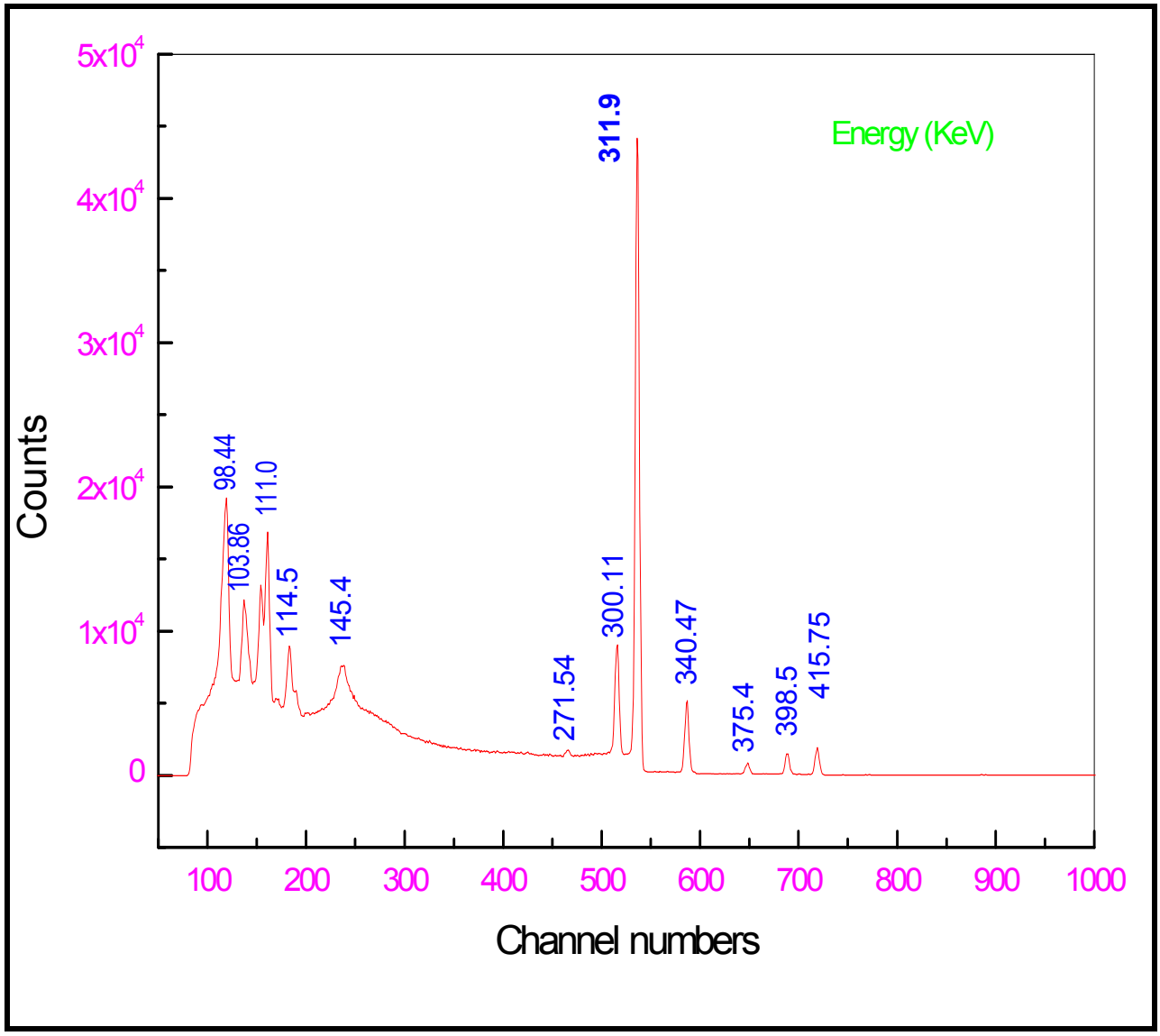

Fig. 5.2 Gamma-ray spectrum of radiochemically separated ^{233}Pa showing seven different γ- rays with their branching intensities with x-axis as channel numbers

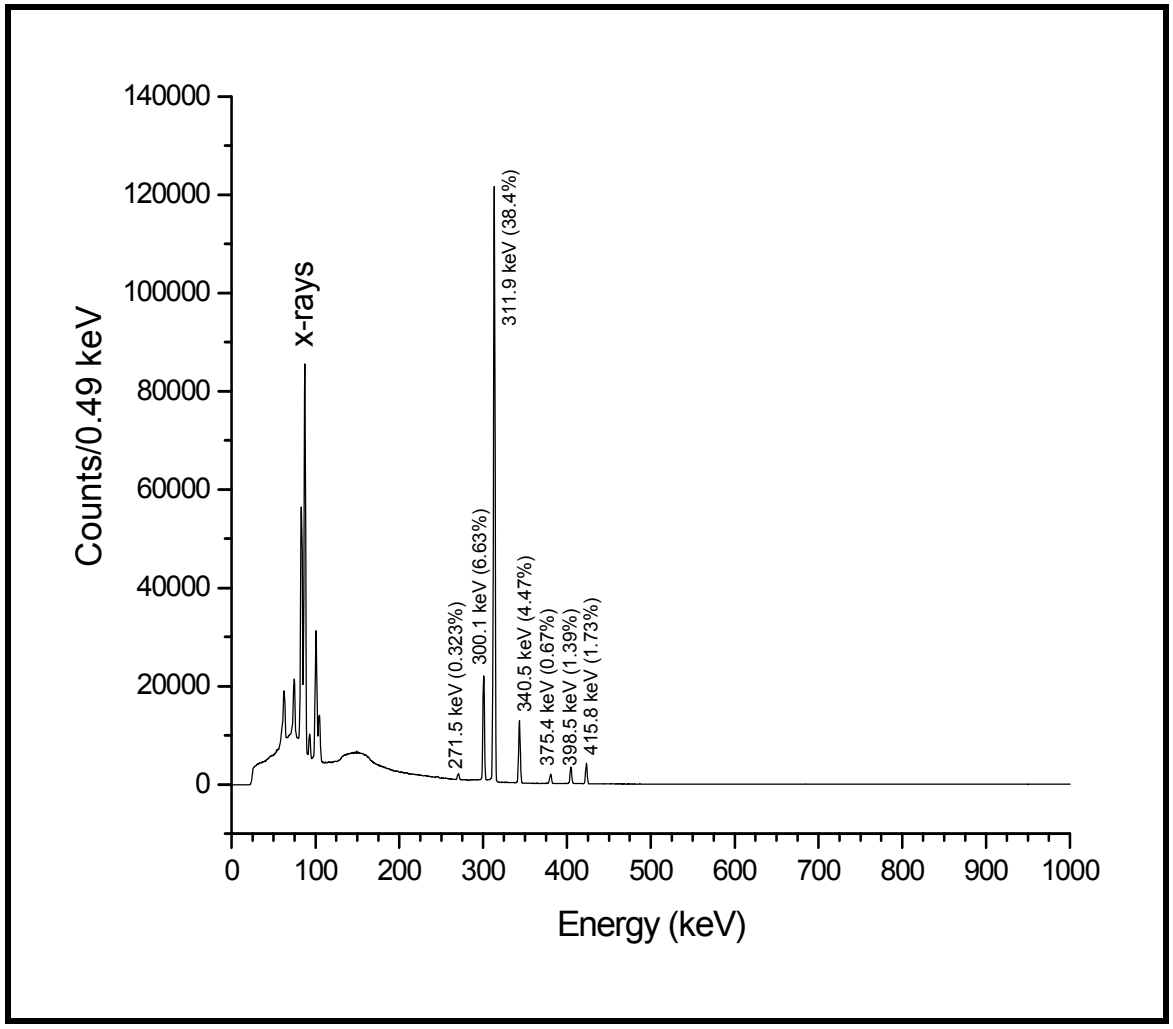

Fig. 5.3 Gamma-ray spectrum of radiochemically separated ^{233}Pa showing seven different γ- rays with their branching intensities with x-axis as Energy (keV)

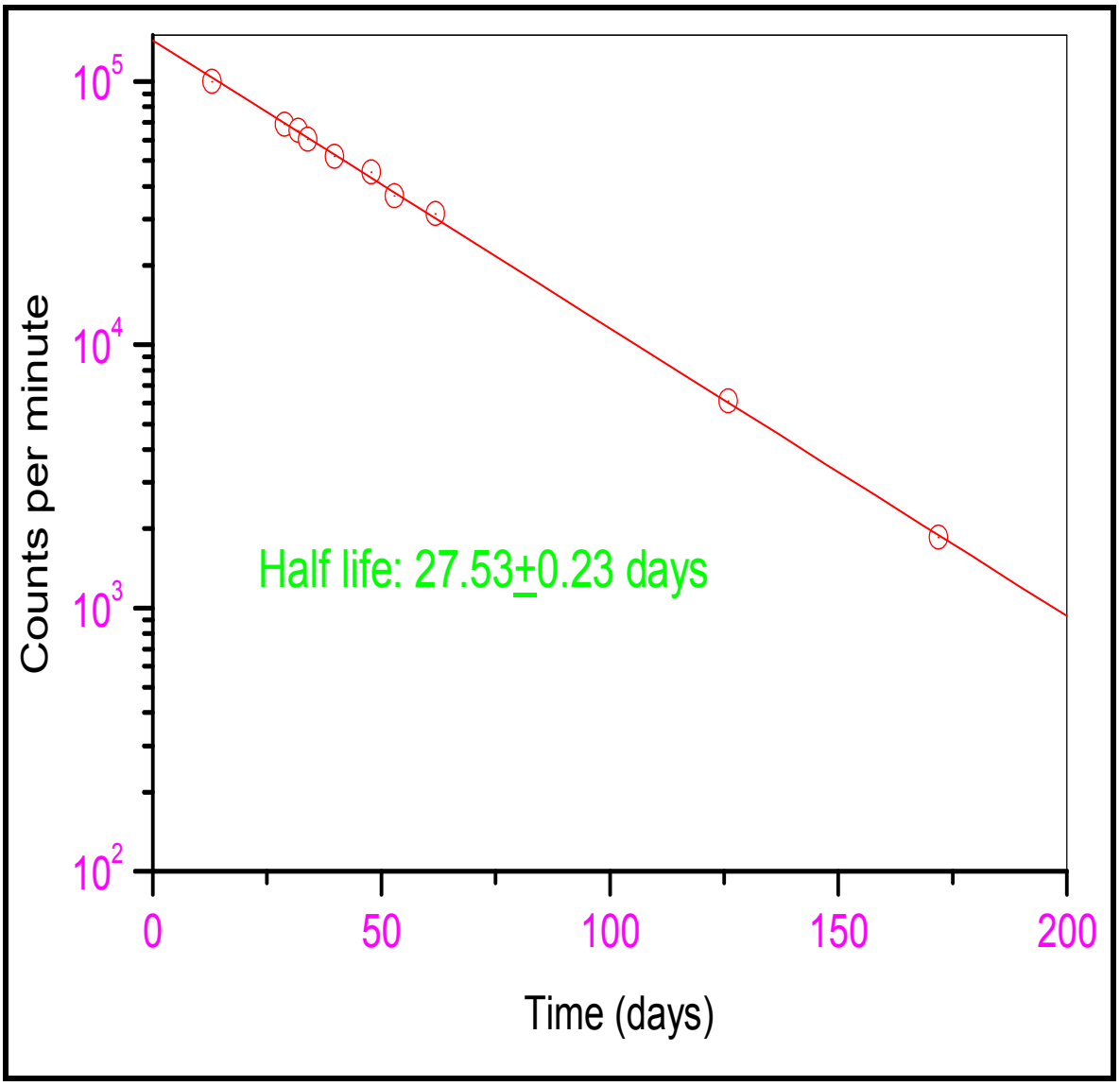

Fig. 5.4 Radioactive decay of the ^{233}Pa as a function of time

5.3.2 ^{233}Pa sample preparation

The separated solution of ^{233}Pa in the chloride medium was evaporated to dryness several times with nitric acid to eliminate chloride. Finally 5.2 ng of ^{233}Pa in the form of nitrate was dried on a 0.025 mm thick aluminum foil. Dried $^{233}Pa(NO_3)_3$ was covered with a 0.0075 mm thick Lexan foil of size 1.5 cm x 1.5 cm. This is bigger than the active sample area of size 1.3 cm x 1.3 cm. The target/detector assembly was wrapped with additional aluminum foil and doubly sealed with alkathene. Similarly 0.0218 grams of a gold metal piece of 0.025 mm thick was also doubly sealed with alkathene. The ^{233}Pa target/detector assembly and the gold sample were kept together inside a polypropylene tube container and irradiated in the reactor APSARA for 8 h. Irradiation was done immediately to eliminate the ^{233}U production from the decay of its precursor ^{233}Pa. The irradiated target/detector assembly of ^{233}Pa was cooled over night. However, the irradiated gold target after few hours of cooling was used for γ-ray spectrometric analysis to determine the thermal neutron flux. The γ-ray counting of the irradiated gold target was done for the 411.8 keV γ-line of ^{198}Au using same 80 cm^3 HPGe detector coupled to the PC-based 4K-channel analyzer.

5.3.3 Calculations

From the photo-peak activity of the 411.8 keV γ-ray of ^{198}Au, the number of detected γ-rays (A_{obs}) was obtained after Compton background subtraction. The number of detected γ-ray activity (A_{obs}) related to the thermal neutron flux (Φ) with the following relation

$$Aobs\left(\frac{CL}{LT}\right) = N\sigma\varphi a\varepsilon\,(1 - e\,(-\lambda t)e(-\lambda T)(1 - e(\lambda CL)/\lambda \qquad (1)$$

where 'n' is the number of targets atom of ^{197}Au, σ is the thermal neutron activation cross-section and 'a' is the branching intensity of the 411.8 keV γ-line of ^{198}Au. 'ε' is the absolute photo-peak efficiency of the detector system for the 411.8 keV γ-line of ^{198}Au, which was obtained by using a standard ^{152}Eu source. 't' and T are the irradiation time and cooling time, whereas CL and LT are clock time and live time of counting, respectively. 'λ' is the decay constant and is related to the half-life ($T_{1/2}$) of the radionuclide with the relation ($\lambda = 0.693/T_{1/2}$).

The $^{197}Au(n,\gamma)$ ^{198}Au reaction cross-section (σ) from Ref. [19] and γ-ray abundance (a) from Ref. [11] were used in Eq. (1) to calculate the thermal neutron flux (Φ) of the irradiation position. It was found to be 1.2 x 10^{12} n cm^{-2} s^{-1}, which is in good agreement with the value earlier used by us in Ref. [25].

For the calculation of the $^{233}Pa(2n_{th}, f)$ cross section, the irradiated Lexan nuclear track detector of the ^{233}Pa was removed and washed with water. It was then etched in 6 N NaOH at 60 ^0C for one hour and the developed fission tracks were counted under an optical microscope at a magnification of 500x [26]. The counting of fission tracks within a few fields i.e. fraction of the total area was done by visual inspection under the microscope. A typical fission track developed on the Lexan detector is given in Fig. 5.5 (a) and (b) from which the elliptical shape of fission tracks of ca. 15 μm size can be clearly seen. Fig. 5.5 (a) and (b) show different areas of the same slide counted and taken the image in two different microscopes, using the same magnification. The structures other than the small elliptical shapes seen in Fig. 5 (a) and (b) are background features. For example, the broad feature of top right in Fig. 5 (a) and small circular faint dots are the background. The visual counting of the fission track by microscope can cause a systematic error of about 1%.

From the measured track density, T_d ($1.74x10^3$ cm^{-2}) and total area, Ω (cm^2) of the Lexan foil (1.69 cm^2), the total number of fission (F) occurring from $^{233}Pa(2n_{th}, f)$ was calculated as [26]

$$F = n\sigma_f \Phi t = T_d \Omega / K_{dry}; \quad \sigma_f = T_d \Omega / n\Phi t K_{dry} \qquad (2)$$

where n = total number of ^{234}Pa target atoms i.e. 1.837 $x10^7$ atoms produced from 5.2 ng of ^{233}Pa during 8 h of irradiation.

σ_f = fission cross-section (cm^2)

Φ = neutron flux = 1.2 x 10^{12} n cm^{-2} s^{-1}

t = irradiation time (s) = 28800 s

K_{dry} = efficiency factor for track registration in Lexan from the target in 2л geometry and taken as 0.958 [26].

All the above values were used in Eq. (2) to calculate the $^{233}Pa(2n_{th}, f)$ i.e $^{234}Pa(n_{th},f)$ cross section.

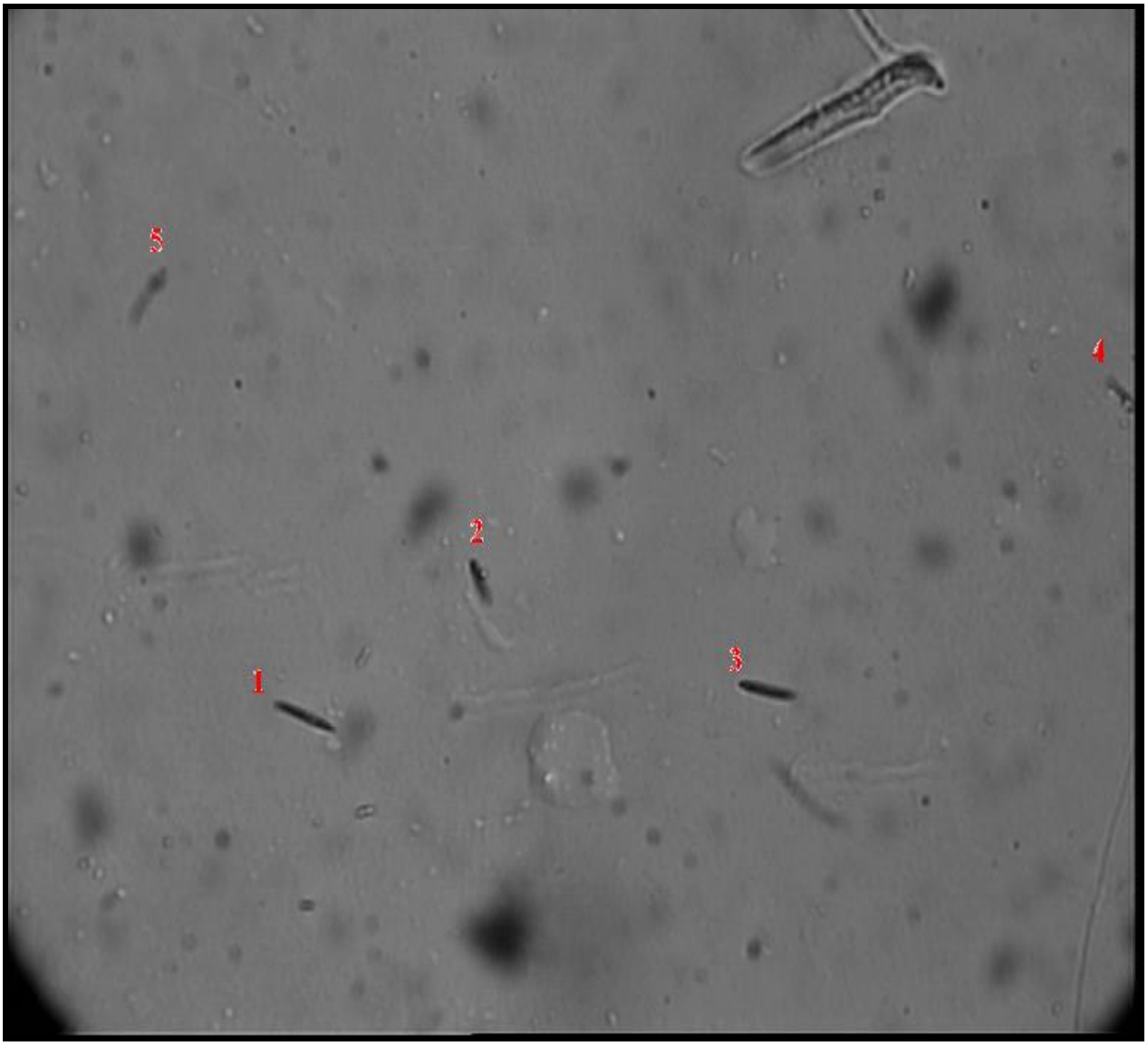

Fig. 5 (a)

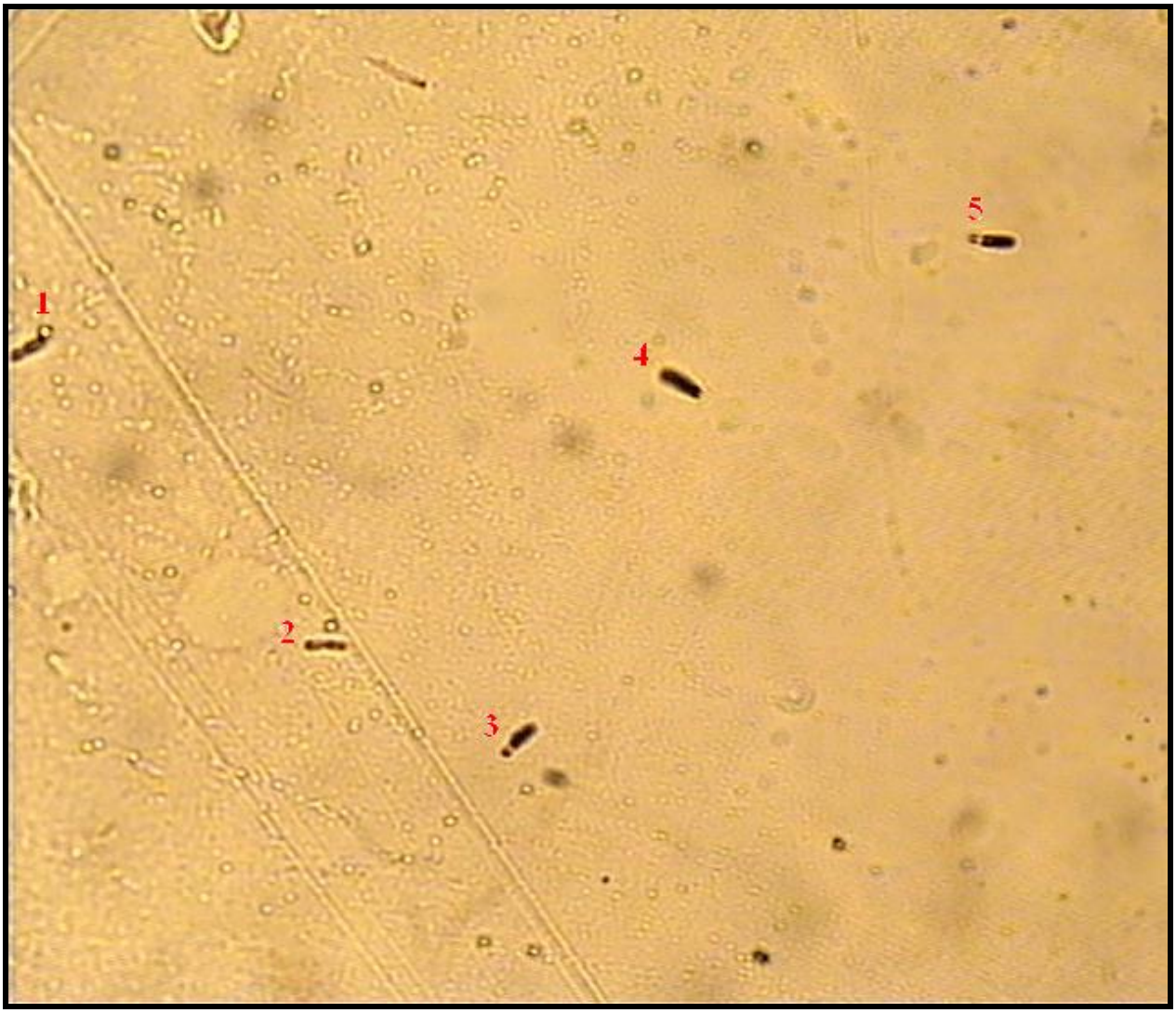

Fig. 5 (b)

Fig. 5 (a), (b) Fission tracks of ca. 15 µm size with elliptical shapes from $^{233}Pa(2n_{th}, f)$, recorded and developed on the Lexan detector with 500x magnification. Figs. 5 (a) and 5(b) correspond to different areas of the same slide and the image was taken with different microscopes using the same magnification. The size of the magnified view of the track area of the lexan detector shown in (a) and (b) are 0.00159 cm^2.

5.4 Results and Discussion

The $^{233}Pa(2n_{th}, f)$ cross-section (σ_f) was calculated from Eq. (2) and found to be 4834±57 barns, which is significantly high. The error quoted for the $^{233}Pa(2n_{th}, f)$ cross section is based on the replicate measurement, which is about 1.2%. Other systematic errors are due to neutron flux (0.5%), irradiation time (0.2%) and visual counting of the fission track under microscope (1%), which was mentioned before. Thus, the total systematic error is around 1.8%.

To the best of our knowledge, there is no data available in literature for the thermal neutron induced fission cross-section of ^{234}Pa except an upper limit of <500 barns for $^{234}Pa^m$ and <5000 barns for $^{234}Pa^g$ quoted in Ref. [19]. So the experimentally obtained thermal neutron cross-section of 4834±57 barns for ^{234}Pa ($^{233}Pa(2n_{th}, f)$) from the present work has been determined for the first time. However, from the present experiment, it is not possible to determine the individual thermal neutron fission cross section of $^{234}Pa^m$ and $^{234}Pa^g$, separately. The fission cross section of 4834±57 barns for $^{234}Pa(n_{th}, f)$ (i.e. $^{233}Pa(2n_{th}, f)$) is significantly higher than the 700 barns for $^{232}Pa(n_{th}, f)$ (i.e. $^{231}Pa(2n_{th}, f)$) [19]. The unusually high cross section of $^{234}Pa(n_{th},f)$ is comparable to the fission cross section [19] of 2088 barns for $^{238}Np(n_{th}, f)$ (i.e. $^{237}Np(2n_{th},f)$) and 6950 barns for $^{242}Am^m(n_{th},f)$ (i.e. $^{241}Am(2n_{th},f)$), respectively.

The fission cross section of $^{232}Pa(n_{th}, f)$, $^{238}Np(n_{th}, f)$ and $^{242}Am(n_{th}, f)$ were theoretically calculated by A.J. Koning et al. [27] using the TALYS computer code [28]. Their calculation reproduces the experimental value after extrapolation to the thermal energy region and normalizing (uplifting) the graph. However, the fission cross section of $^{234}Pa(n_{th}, f)$ reported by Koning et al. [27] using the TALYS code is very low. The normalization of the TALYS value for $^{234}Pa(n_{th}, f)$ was not done by Koning et al [28] unlike in the cases of $^{238}Np(n_{th}, f)$ and $^{242}Am(n_{th}, f)$ due to the unavailability of experimental data in the former case. Among the above fissioning systems, $^{241}Am(2n_{th}, f)$ has an unusually high fission cross section similar to the fissioning system $^{233}Pa(2n_{th}, f)$. In view of this, $^{233}Pa(2n_{th}, f)$ and $^{241}Am(2n_{th}, f)$ cross sections were calculated theoretically using the TALYS computer code version 1.2 in a similar way as done by Koning et al .

TALYS can be used to calculate the reaction/fission cross section based on a physics model and parameterizations. It can be used for the nuclear reaction/fission that involves targets of A≥12 and projectiles like photon, neutron, proton, ^{2}H, ^{3}H, ^{3}He and alpha particles in the energy range of 1 keV to 200 MeV. In the present work, we have used neutron energies from 1 keV to 20 MeV for ^{234}Pa and ^{242}Am targets. All possible outgoing channels for a given projectile (neutron) energy were considered. However, the cross section for the (n, f) reaction was specially looked for and collected. The pre-equilibrium contribution to the reaction cross section was considered beyond the excitation energy of 22.0 MeV (beyond 203 discrete levels). Theoretically calculated $^{234}Pa(n, f)$ and $^{242}Am(n, f)$ reaction cross sections from neutron energies of 1 keV to 20 MeV were plotted in Figs. 5.6 and 5.7, respectively. It is not possible to calculate the fission cross section theoretically by the TALYS computer code in the lower energy region down to thermal energies. Thus the theoretical value was extrapolated by using a 1/v law to the lower energy region for ^{242}Am (Fig. 5.7).

The extrapolated theoretical values in the thermal region are much lower than the experimental value of 6950 barns [19, 29]. Thus it is necessary to normalize the graph by a factor of about 6.7 to reproduce the experimental thermal neutron induced fission cross section of ^{242}Am. Similarly normalizing the graph by a same factor of about 6.7 in the thermal neutron induced fission of ^{234}Pa reproduces the experimental fission cross section of the present work. Thus the unusually high cross section of 4834 b for $^{233}Pa(2n_{th}, f)$ is justified in analogue to the cross section of 6950 b for $^{242}Am(2n_{th}, f)$.

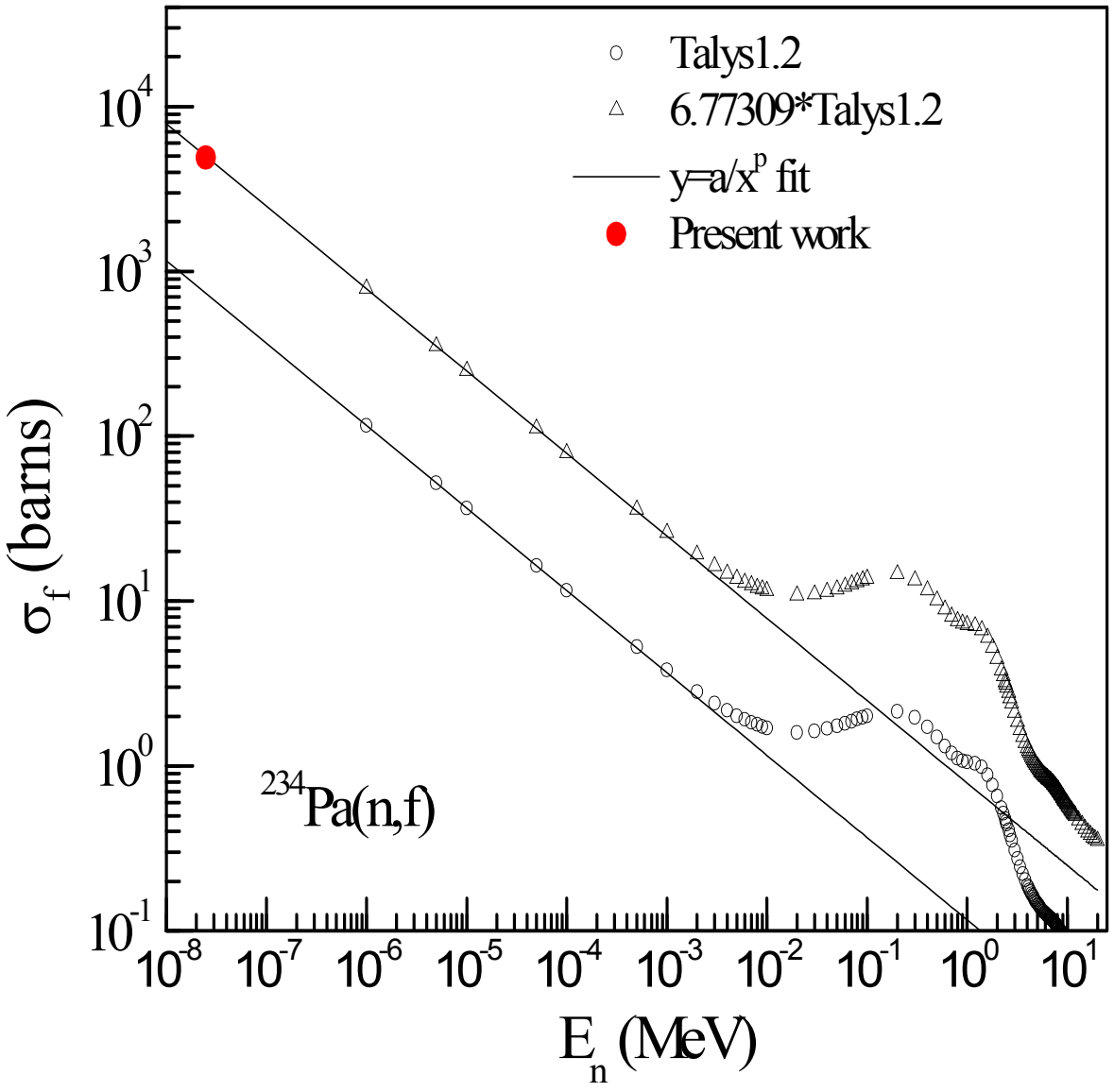

Fig. 5.6 Plot of experimental and theoretically ^{234}Pa(n, f) cross-section. Theoretical fission cross sections above 1 keV were calculated using the TALYS computer code version 1.2. The fission cross-section below 1 keV up to thermal energy was extrapolated by a normalized fit of the 1/v formula as shown in the figure.

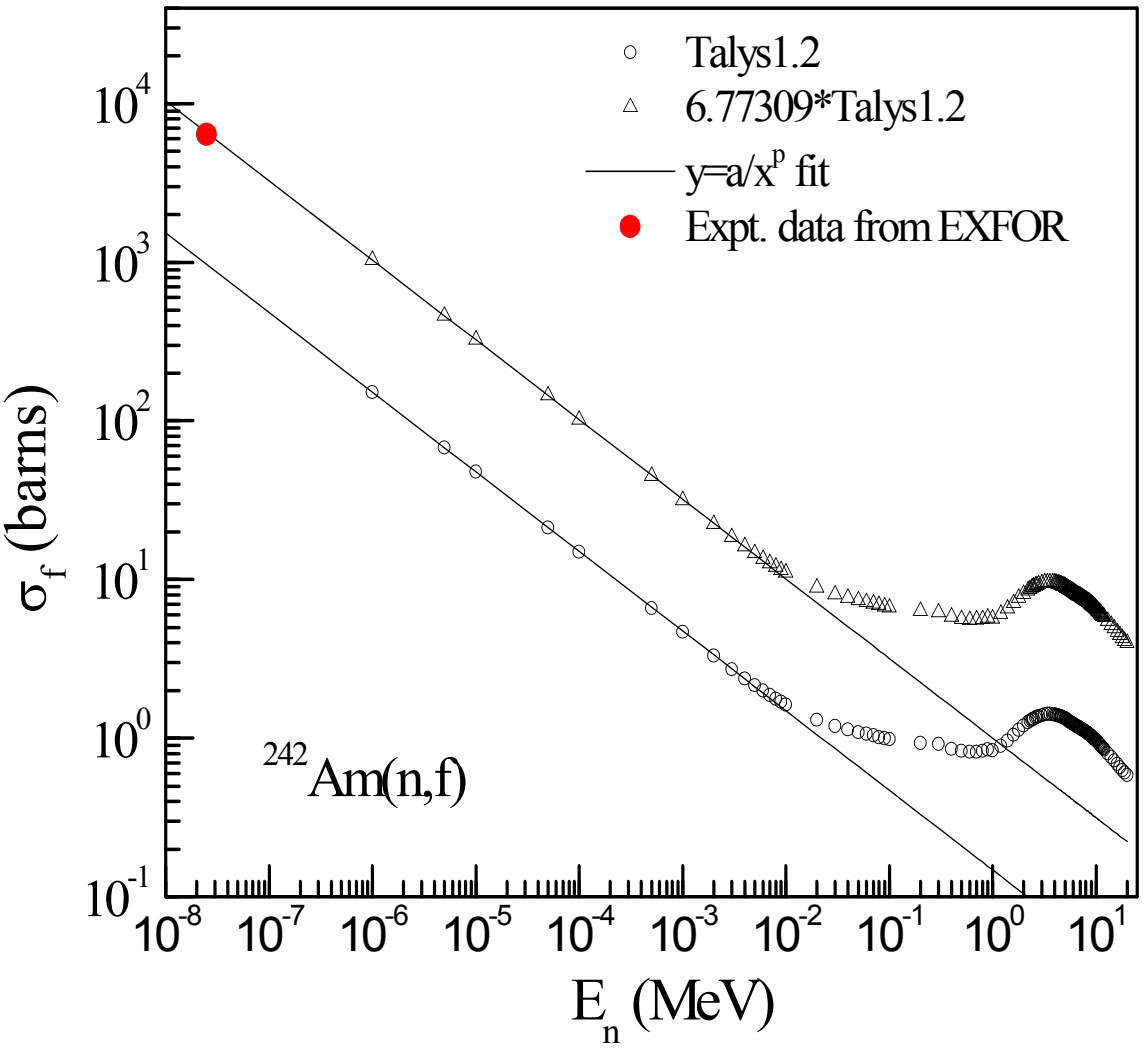

Fig. 5.7 Plot of experimental and theoretically ^{242}Am(n, f) cross-section. Theoretical fission cross sections above 1 keV were calculated using the TALYS computer code version 1.2. The fission cross-section below 1 keV up to thermal energy was extrapolated by a normalized fit of the 1/v formula as shown in the figure.

The cross section of $^{233}Pa(2n_{th}, f)$ is important from the point of view of AHWR and ADS design. This is because ^{233}Pa is a precursor to the fissile material ^{233}U. The equilibrium production of the fissile nucleus ^{233}U depends on the $^{232}Th(n, \gamma)$ and $^{233}Pa(n, \gamma)$ reactions as well as on the $^{233}Pa(n, f)$ and $^{233}Pa(2n_{th}, f)$ cross sections. This is required with an accuracy of 1-2 % to be used safely in simultaneous techniques for predicting the dynamical behavior of the complex arrangements in AHWR and ADS.

5.5 Summary and Conclusion

^{233}Pa is an important intermediary in the thorium based fuel cycle and thus its fission cross section is a key parameter in the modeling of AHWR and ADS. The $^{233}Pa(2n_{th}, f)$ cross-section has been experimentally determined a fission track-technique. The experiment was carried out using APSARA reactor at Bhabha Atomic Research Centre, Mumbai, India. The radiochemical separation of ^{233}Pa from irradiated Thorium Nitrate was performed at Radiochemistry Division, Radiological Lab (RLG), B.A.R.C, Mumbai, India. This is because the ^{233}Pa is an important intermediary in the thorium based fuel cycle and thus its fission cross section is a key parameter in the modeling of AHWR and ADS. The following conclusions have been drawn from this work.

1. The $^{233}Pa(2n_{th}, f)$ cross-section has been experimentally determined for the first time using a fission track-technique. It was found to be 4834±57 barns.

2. The $^{233}Pa(2n_{th}, f)$ cross-section was found to be 4834±57 barns, which is significantly high and thus it is very important for ^{232}Th-^{233}U based fuel in advanced heavy water reactors (AHWR) and accelerator driven sub-critical systems (ADS).

3. The $^{233}Pa(2n_{th},f)$ cross section was calculated theoretically using the TALYS computer code and found to be in good agreement with the experimental value after normalization with respect to $^{241}Am(2n_{th}, f)$.

4. The $^{233}Pa(2_{nth}, f)$ fission cross-section has immense importance from a neutronics and physics point of view for the design of AHWR and ADS.

References

[1]. T.R. Allen and D.C. Crawford, Science and Technology of Nuclear Installations, Article ID 97486 (2007)

[2]. P.E. MacDonald, N. Todreas, Annual Project Status Report 2000, MIT-ANP-PR-071, INEFL/EXT-2009-00994

[3]. R.K. Sinha and A. Kakodkar, "Design and Development of AHWR – The Indian Thorium Fueled Innovative reactor," Nucl. Eng. Des. **236**, 7-8, 683 (2006)

[4]. Fast Reactors and Accelerator Driven Systems Knowledge Base, IAEA-TECDOC-1319: Thorium fuel utilization: Options and Trends

[5]. L. Mathieu et al., "Proportion for a very simple Thorium Molten Salt reactor," Proc. Global International Conference, Paper No. 428, Tsukuba, Japan, 2005

[6]. S. Ganesan, "Creation of Indian Experimental Benchmarks for Thorium Fuel Cycle," IAEA Coordinated research project on "Evaluated Data for Thorium- Uranium fuel Cycle," Third Research Co-ordination Meeting, 30 January to 2 February 2006, Vienna, Austria, INDC (NDS) - 0494 (2006)

[7]. F. Carminati et al, "An Energy Amplifier for Cleaner and Inexhaustible Nuclear Production Driven by Particle Beam Accelerator," CERN/AT/93-47 (ET) 1993

[8]. C. Rubbia et al, "Conceptual Design of a Fast Neutron Operated High Power Energy Amplifier," CERN/AT/95-44 (ET)1995

[9]. Accelerator Driven Systems: Energy Generation and Transmutation of nuclear waste, Status report: IAEA- TECDOC- 985 (Nov. 1997)

[10]. S. Ganesan, Pramana, J. Phys. **68**, 257 (2007)

[11]. R.B. Firestone and L.P Ekstrom (2004), Table of radioactive isotopes Vol 2. http://ie.lbl.gov/toi/index.asp.

[12]. J. Halperin et al, Nucl. Sci. Eng. **1**, 1 (1956)

[13]. S. Boyer et al., Nucl. Phys. A **775**, 175 (2006)

[14]. H.R. von Gunten, R.F. Buchanan, and K. Behringer, Nucl. Sci. Eng. **27**, 85 (1967)

[15]. F. Toversson et al., Phys. Rev. Let. **88**, 062502-1 (2002)

[16]. F. Toversson, et al., Nucl. Phys. A **733**, 3 (2004)

[17]. M. Petit et al., Nucl. Phys. A **735**, 345 (2004)

[18]. B.K. Nayak et al., Phys. Rev. C **78**, 061602 (2008)

[19]. S.F. Mughabghab, M. Divadeenam and N.E. Holden, Neutron Resonance and Thermal Cross Sections, Vol I, Academic Press, New York (1981)

[20]. R. Vandenbosch and J.R. Huizenga, Nuclear Fission, Academic Press, New York (1973)

[21]. C. Wagemans, The Nuclear Fission Process, CRC Press, London (1990).

[22]. "50 Glorious Years of APSARA", http://www.barc.gov.in/publications/tb/apsara.pdf

[23]. P.N. Pathak, R. Veeraraghavan, P.B. Ruikar and V.K. Manchanda, Radiochim. Acta **86**, 129 (1999).

[24]. A.K. Pandey, H. Naik, R.J. Singh, A. Ramaswami, P.C. Kalsi, A.G.C. Nair and R.H. Iyer, Radiochim. Acta 87, 1 (1999).

[25]. H. Naik, S.P. Dange and R.J. Singh, Phys. Rev. C **71**, 014304, 2005

[26]. H.A. Khan and S.A. Durrani, Nucl. Inst. Methods **98**, 229 (1972)

[27]. A.J. Koning and D. Rochman, TENDL-2009: "TALYS- based Evaluated Nuclear Data Library", at www.talys.eu/tendl-2009/

[28]. A.J. Koning, S. Hilaire and M.C. Duijvestijn, Proceeding of the International Conference on Nuclear Data for Science and Technology- ND 2004, AIP Vol.769, Edited by R.C. Haight, M.B. Chadwick, T. Kawano and P. Talou (Santa Fe, 2005), Page No. 1154

[29]. "The EXFOR/CSISRS Database" http://www-nds.iaea.org.